Scientia Iranica B (2012) 19 (5), 1288–1298

Sharif University of Technology

**Scientia Iranica**

*Transactions B: Mechanical Engineering*

www.sciencedirect.com

# Nano cluster manipulation success considering flexibility of system: Coarse grained molecular dynamics simulations

**M.H. Korayem** *, **V. Rahneshin, S. Sadeghzadeh**

*Robotic Research Laboratory, Center of Excellence in Experimental Solid Mechanics and Dynamics, School of Mechanical Engineering, Iran University of Science and Technology, Narmak, Tehran, 16846, Iran*

Received 12 January 2012; revised 6 May 2012; accepted 19 June 2012

**KEYWORDS**

Nano cluster;
Nano manipulation;
Molecular physics;
Coarse Grained Molecular Dynamics (CGMD);
Tip flexibility.

**Abstract** In this paper, the results of using a Coarse Grained Molecular Dynamics (CGMD) model to simulate the process of manipulation of nano clusters with a flexible tip are reported, and the reasons for some failures are discussed. After comparison of these results with those from a macro model, some failures of the nano manipulation process, due to damage, fracture, or crushing of tip, substrate, and nano cluster, are examined. At the end, after a parametric study of nano cluster deformations, the use of the tip cluster, $\varepsilon_p$-SP diagram, for optimal selection of the tip material, is discussed.



## 1. Introduction

Since the introduction of Scanning Probe Microscopes (SPMs), especially Atomic Force Microscopes (AFMs), they have been utilized as efficient robots in the nano scale world. In this regard, SPMs were first used in surface lithography and later as a device for manipulating the nano objects, including nano particles, nano wires, nano rods, and nano tubes, etc. The processing time of nanometric systems varies from several nanoseconds to several microseconds. Therefore, even the powerful Molecular Dynamics (MD) method has some difficulties in simulating such processes, since it is limited to time intervals of the order of a femtosecond. In this situation, the existence of different sources of error tends to a significant deviation in the desired results. Introducing an exact and appropriate computational method, capable of simulating both large and small scales of the manipulation system, is one of the best methods for the compensation of these errors. Use of the method of CGMD remedies these problems to some extent.

Typically, classical models have many limitations when applied. Despite their low computational costs, continuum based methods are incapable of describing different phenomena in nano scale fields. On the other hand, molecular dynamics models are limited with respect to the time scale [1,2]. For this reason, modeling in the order of micro meter and micro second is only possible by supercomputers. Therefore, researchers are in search of some comprehensive synthetic methods which have the advantages, but not the drawbacks, of the original methods. The outcome of this research work has been the introduction of multi scale methods [3]. The main concern in the simulation of multi scale systems is to provide an appropriately exact model for both the large and small scale environments, based on continuum mechanics and molecular dynamics, respectively. There has been much work in the area of continuum based problems on increasing the precision of the proposed models [4–6]. However, there are still many obstacles in molecular dynamics simulations for studying the nano scale domain. This fact can be clearly observed by focusing on nano manipulation researches.

Sitti has surveyed nano manipulation systems in [7]. In his work, some nano manipulation strategies are grouped according to their starting point, utilized process, operation type, manipulation environment, interaction type, etc. The dynamic behavior of nano particle motion during nano probe based manipulation is investigated in [8,9]. Zhang et al. used an active atomic force microscope probe to control the tip position by changing the cantilever's flexibility or rigidity through different control strategies in imaging and

* Corresponding author. Tel.: +98 21 77240540 50; fax: +98 21 77240488.
*E-mail addresses:* hkorayem@iust.ac.ir (M.H. Korayem), wahid65r@gmail.com (V. Rahneshin), Sadeghzadeh@iust.ac.ir (S. Sadeghzadeh).

Peer review under responsibility of Sharif University of Technology.

Production and hosting by Elsevier

1026-3098 © 2012 Sharif University of Technology. Production and hosting by Elsevier B.V. All rights reserved.
doi:10.1016/j.scient.2012.06.022

**Nomenclature**

| | |
|---|---|
| $H_I^{RTS}$ | Potential for the binary A B dissimilar materials |
| $V\left(r_{ij}\right)$ | A pair wise repulsive interaction between atoms $i$ and $j$ |
| $\rho_i^A, \Phi^A, \Phi^{AA}, \Phi^{AB}, \rho_i^B, \Phi^B, \Phi^{BB}, V^{xy}(r), \Phi^{xy}(r)$ | Parameters of RTS potential energy |
| $r_{ij}$ | Distance between $i$th and $j$th atom |
| $\hat{p}_i$ | The site occupancy operator |
| $d^{xy}, \varepsilon^{xy}, C^{xy}, m^{xy}, n^{xy}, a^{xy}$ | Constants of potential energy for body $x$ and $y$ |
| $\varepsilon$ | Energy parameter of potential energy |
| $a$ | Length parameter of potential energy |
| '$m$' and '$n$' | Positive constants in potential energy |
| $U$ | Internal potentials |
| $F_i$ | External forces |
| $t$ | Current time |
| $t + \Delta t$ | Time at next time step |
| $v$ | Velocities |
| $r(t)$ | Positions of atoms at time '$t$' |
| $r(t + \Delta t)$ | Positions of atoms at time '$t + \Delta t$' |
| $T_0$ | Desired system temperature |
| $T_i$ | Temperature in $i$th time step. |
| $F_{z0}$ | Normal preload force |
| $Z_{P0}$ | Normal deflection offset |
| $FT$ | Pushing force |
| $m$ | The nominal mass of atoms in MD |
| $L$ | Nominal distance of atoms in MD |
| $m_c$ | The nominal mass of atoms in CGMD |
| $L_c$ | Nominal distance of atoms in CGMD |
| SP | Success Parameter |
| $R_a$ and $R_b$ | The large and small diameters of the nano cluster, |
| $\varepsilon_p$ and $\varepsilon_t$ | The parameters of Sutton–Chen potential for nano cluster and tip. |

manipulation modes, respectively [10]. The main challenge faced by nanomanipulation systems seems to be the surface interaction of substrate/particle, and manipulator/particle. The contact deformation and molecular attraction of a ball and a surface have been developed in [11]. Quesne et al. [12] have utilized the generalized form of the Lennard-Jones soft-sphere pair potential to examine the adhesional behavior of particles on surfaces for different materials. The interactions of some different clusters of pure Ag, pure Au, and mixed Ag Cu with the surface have been investigated in [13]. Then, using the tip of a scanning tunneling microscope, the manipulation of these particles on the surface has been performed. In [14], scanning tunneling microscopy is used to study the adsorption and manipulation of single molecules on Cu. Applying both the continuum mechanics and molecular mechanics simulations, Hertel and Robert investigated the strength and effect of surface van der Waals forces on the shape of multi-walled and single-walled carbon nanotubes, using the atomic force microscopy [15]. In [16], some micromanipulations have been simulated using only the adhesion forces; in this work, based on the hypothesis that Newton's laws are applicable to this scale, dynamic models of a simple task, consisting of picking up and placing micro spheres, are proposed. Although there is extensive work available on nano manipulation, this subject still remains one of the most challenging issues confronted by the world of molecular dynamics research.

In the molecular models, all the atoms of a particular material react through inter atomic potentials. These models are capable of simulating the ultra fine structures of materials in nano scale. There has been much work concerning the application of molecular dynamics in the nano manipulation process. Some mechanisms of the adsorption of gold clusters on Ni and Au surfaces have been investigated by means of molecular dynamics simulations [17]. In addition, some recent works have focused on the dynamic behavior of manipulation systems using the AFM tip as a manipulator. Mahboobi et al. [18] investigated the effects of material type and manipulation strategy on the success of the nano manipulation process by planar molecular dynamics. He later used MD simulations to study the manipulation of metallic nano clusters, and the effects of material type and manipulation strategy on the success of the process [19]. Despite the aforementioned, the development of models that are capable of simulating more comprehensive conditions is still a high priority among the researchers of molecular dynamics issues.

The aim of this paper is to introduce a more comprehensive model for the manipulation of the nano cluster. Therefore, a planar coarse grained molecular dynamics model covering tip flexibility is proposed. Newtonian mechanics is employed, and the Sutton–Chen potential and its extended form, Rafii Tabar–Sutton, are used. For validation of the proposed model, the results have been compared with those of previous work in [20,21]. To study the success of manipulation results, qualitatively and quantitatively, different failures of the manipulation process are presented and studies are conducted on the effect of different parameters on the deformation of the nano cluster. Finally, the optimal selection of nano cluster and tip, which results in the most exact positioning, is discussed.

The technical aspects of the simulation details are stated in the following sections and can be also comprehensively found in [22].

## 2. Molecular dynamics

In order to establish the relations of molecular dynamics for a system of particles, some parameters are required. Particle mass, initial position of atoms, initial velocity of atoms, potential energy between the atoms and external force fields, and the equations of motion are five effective parameters that must be determined for the system in order to have a unique solution [23].

In a state of equilibrium, atoms can have different arrangements based on the material phase. It is common for the atoms of gases and liquids not to have a specific structure. Contrary to gases and liquids, solids possess a higher potential energy level relative to the kinetic energy. The atoms of solids, especially of metals, usually form specific lattice configurations. For metals, there are two types of solid lattice that are more common, namely, Face-Centered Cubic (FCC) and Body-centered Cubic (BCC) lattices. In the current work, the FCC lattice is applied for the metal atoms to represent the initial positions.

A classical MD simulation is constructed by introducing a finite nano-sized cell, including $N$ atoms, of an infinite model system with any desired configuration. The cell is replicated in all planar dimensions, generating its own periodic images as well as those of the original $N$ atoms. This is "the Periodic Boundary Condition" (PBC), which is used in MD simulations [24]. Also, in order to carry out atomic simulations, a way of expressing atomic rules is inevitable. In computer simulations, these rules are known as "inter atomic potential

energy". For the simulation of a metal system, the simple two body potentials, like those of Lenard Jones, are not intelligent choices, as they lack the desired capability to encompass all the physical properties of metals. Therefore, the Rafii Tabar–Sutton multi body long range potential, which is an extended form of the Sutton–Chen potential and capable of modeling the interactions of dissimilar materials, is used in the current study. The general form of the Rafii Tabar–Sutton (RTS) potential for the binary A–B dissimilar materials is [24,25]:

$$H_I^{RTS}Z = \frac{1}{2}\sum_i \sum_{j\neq i} V\left(r_{ij}\right) - d^{AA}\sum_i \hat{p}_i\sqrt{\rho_i^A} - d^{BB}\sum_i (1-\hat{p}_i)\sqrt{\rho_i^B}, \quad (1)$$

with:

$$V\left(r_{ij}\right) = \hat{p}_i\hat{p}_j V^{AA}\left(r_{ij}\right) + \left(1-\hat{p}_i\right)\left(1-\hat{p}_j\right)V^{BB}\left(r_{ij}\right) + \left[\hat{p}_i\left(1-\hat{p}_j\right) + \hat{p}_j\left(1-\hat{p}_i\right)\right]V^{AB}\left(r_{ij}\right), \quad (2)$$

$$\rho_i^A = \sum_{j\neq i}\Phi^A\left(r_{ij}\right) = \sum_{j\neq i}\left[\hat{p}_j\Phi^{AA}\left(r_{ij}\right) + \left(1-\hat{p}_j\right)\Phi^{AB}\left(r_{ij}\right)\right], \quad (3)$$

$$\rho_i^B = \sum_{j\neq i}\Phi^B\left(r_{ij}\right) = \sum_{j\neq i}\left[\left(1-\hat{p}_j\right)\Phi^{BB}\left(r_{ij}\right) + \hat{p}_j\Phi^{AB}\left(r_{ij}\right)\right]. \quad (4)$$

Function $V(r_{ij})$ is defined between atoms $i$ and $j$, separated by distance $r_{ij}$. $\hat{p}_i$ in the above equations is defined as:

$$\hat{p}_i = \begin{cases} 1 & \text{if site } i \text{ is occupied by an A atom} \\ 0 & \text{if site } i \text{ is occupied by an B atom.} \end{cases} \quad (5)$$

The functions $V^{xy}(r)$ and $\Phi^{xy}(r)$ are defined as:

$$V^{xy}(r) = \varepsilon^{xy}[a^{xy}/r]^{n^{xy}}, \quad (6)$$

$$\Phi^{xy}(r) = [a^{xy}/r]^{m^{xy}}, \quad (7)$$

and the constants are expressed as:

$$d^{AA} = \varepsilon^{AA}C^{AA}, \qquad d^{BB} = \varepsilon^{BB}C^{BB},$$

$$m^{AB} = \frac{1}{2}(m^{AA}+m^{BB}), \qquad n^{AB} = \frac{1}{2}(n^{AA}+n^{BB}),$$

$$a^{AB} = \sqrt{a^{AA}a^{BB}}, \qquad \varepsilon^{AB} = \sqrt{\varepsilon^{AA}\varepsilon^{BB}}. \quad (8)$$

In the above relations, $a$ is normally taken to be the equilibrium lattice constant, and '$m$' and '$n$' have the relation $n > m$. The RTS potential has the advantage that all its parameters can be easily obtained from the Sutton–Chen (SC) elemental parameters of metals. Table 1 lists the SC parameters for some metals:

Table 1: Parameters of the Sutton–Chen potential [25].

| Element | $m$ | $n$ | $\varepsilon\ (eV)$ | $c$ |
|---|---|---|---|---|
| Ni | 6 | 9 | 1.5707E−02 | 39.432 |
| Pt | 8 | 10 | 1.9833E−02 | 34.408 |
| Au | 8 | 10 | 1.2793E−02 | 34.408 |
| Ag | 6 | 12 | 2.5415E−03 | 144.41 |
| Cu | 6 | 9 | 1.2382E−02 | 39.432 |
| Ir | 6 | 14 | 2.4489E−03 | 334.94 |
| Pb | 7 | 10 | 5.5765E−03 | 45.778 |
| Pd | 7 | 12 | 4.1790E−03 | 108.27 |
| Rh | 6 | 12 | 4.9371E−03 | 144.41 |

### 2.1. Equations of motion

To describe motion in a multi particle system, normally, the Lagrangian, Hamiltonian, and Newtonian descriptions are used. The Newtonian formulation (i.e. Newton's second law) states that the sum of the internal forces ($\nabla_i U$) and external forces ($F_i$) exerted on every particle is equal to the inter atomic force applied to that particle ($m_i\ddot{r}_i$):

$$m_i\ddot{r}_i + \nabla_i U = F_i^{\text{ext}}. \quad (9)$$

The first term in the above equation denotes the kinetic energy. The second term is an interpretation of potential energy, which is related to the inter atomic potential. The external forces include the force due to the friction of the body with the surrounding environment and the force exerted on the system to change its shape, which belong to the non conservative forces.

Using the Velocity Verlet computational algorithm, the equations of motion can be solved numerically for the system of particles, and the positions and velocities of each single atom can be calculated in desired time steps. In the current study, the time step is set to 80 fs.

### 2.2. Solution procedure

The common method for solving differential equations of motion in molecular dynamics is the well known Finite Difference Method (FDM). Knowing the positions, velocities and other essential data of the system at time '$t$', the goal of the FDM is to calculate these parameters for the next time step, $t + \Delta t$. Therefore, all the differential equations of motion are solved in a step by step manner. Finite difference based methods utilize the Taylor series for expanding the position function of particles [2,23].

Various finite difference algorithms exist for solving the differential equations of atomic motion. They differ in the way of calculating $\dot{r}$. Since the real nano scale systems consist of numerous numbers of atoms, the simulation procedure must encompass large degrees of freedom to take the real behavior of the system into consideration. Therefore, an algorithm with both low computational costs and good precision is in great demand. The Verlet algorithm is one of the most popular methods among nano mechanics researchers. This algorithm combines the forward and backward Taylor expansions. With some simplifications, the relations for velocities and positions of atoms at time '$t$' are expressed as follows:

$$v(t) = \frac{r(t+\Delta t) - r(t-\Delta t)}{2\Delta t}, \quad (10)$$

$$r(t+\Delta t) = r(t) + \Delta t \times v(t) + \frac{1}{2}(\Delta t)^2 \times a(t) + O(\Delta t^4). \quad (11)$$

In a more advanced form of the Verlet algorithm, known as the velocity Verlet, the velocity is calculated using the half step acceleration.

$$v(t+\Delta t) = v(t) + \Delta t \times a\left(t + \frac{1}{2}\Delta t\right) + O(\Delta t^2). \quad (12)$$

This leads to the final form of the velocity Verlet algorithm as:

$$r_i(t+\Delta t) = r_i(t) + \Delta t \times v_i(t) + \frac{1}{2}(\Delta t)^2 \times a_i(t), \quad (13)$$

$$v_i\left(t+\frac{1}{2}\Delta t\right) = v_i(t) + \Delta t \times \frac{a_i(t)}{2}, \quad (14)$$

$$a_i(t+\Delta t) = \frac{F_i(t+\Delta t)}{m_i}, \quad (15)$$

$$v_i(t+\Delta t) = v_i\left(t+\frac{1}{2}\Delta t\right) + \Delta t \times \frac{a_i(t+\Delta t)}{2}. \quad (16)$$

The velocity Verlet algorithm is the most popular computational method in molecular dynamics simulations. By using the second derivative formula in this method, the computational precision gets to about 4th order. This results in a high computational speed, as well as high precision.

### 2.3. NVT ensemble

In the NVT ensemble, the system under consideration must be invariable in the number of particles ($N$), volume ($V$), and temperature ($T$) [23]. This ensemble is usually used for the simulation of closed systems that just exchange energy with the environment. To realize this ensemble, there must be some ways of making the aforementioned qualities constant. A fixed number of atoms can be realized through periodic boundary conditions (as explained earlier in part 2 of this article). Using the total pressure of the system, its volume can be fixed as well. Temperature stabilization in computer simulations is not an easy task. However, it can be realized in three different ways, namely, the stochastic Langevin type method, the constraint method, and the extended system method [24].

The simple constraint method can be carried out by using a velocity scaling procedure in each time step. This tends to limit the total kinetic energy of the system in order to stabilize the system's initial temperature. This ensemble can be produced as the following:

$$\vec{v}_i \rightarrow s\vec{v}_i, \quad (17)$$

where:

$$s = \sqrt{T_0/T_i}. \quad (18)$$

## 3. The proposed nano manipulation strategy

There exist various strategies for the nano manipulation process in literature [18,19]. The scenarios in this paper, however, are somewhat different. Since, in real manipulation systems, the cluster is manipulated by the lateral side of the tip, a different strategy is considered.

The manipulation process cannot be observed in real time. During the pushing of objects, imaging is impossible, because imaging and manipulation tools are the same. As a solution, the surface and targeted clusters could be imaged before and after the manipulation. Using the obtained images, the positions of clusters relative to the basic reference point can be determined [26]. Due to the lack of real time images, using the force feedback data during the process is crucial for proper manipulation. The manipulation strategy for the pushing of a nano cluster is shown in Figure 1. Using a suitable model, the force feedback data during the manipulation strategy can be calculated accurately.

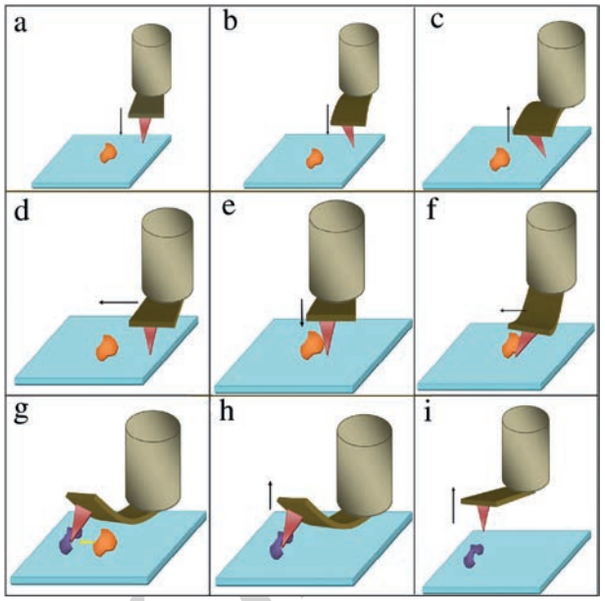


Figure 1: Nano manipulation strategy using the AFM. (a) Auto parking; (b) snap in substrate; (c) pull away from substrate; (d) approach to nano cluster; (e) snap in nano cluster; (f) moving toward the cluster; (g) pushing; (h) pull away from nano cluster; and (i) going to reference point.

In this problem, both the substrate and the nano cluster are stationary at the beginning. Then, the probe moves down to approach the substrate (Figure 1(a)). The Van der Waals force increases until the snap occurs at the point of instability (Figure 1(b)). At this point, the tip jumps to the substrate. This phenomenon can be detected via photodiode data. Then, the tip starts moving upward (Figure 1(c)). Deflection in the cantilever increases until the pulling force overcomes the attraction force (Figure 1(d)). In view of the adhesion force between the tip and substrate, the retraction force is larger than the attraction force. Next, the tip moves reaching the desired cluster, horizontally. Furthermore, the van der Waals force between the tip and cluster increases until the snap to the cluster takes place (Figure 1(e)). Then, the substrate movement follows (Figure 1(f)), and the pushing force on the cluster increases.

The tip may cross the cluster and the process fails. To ensure the desired contact, a small normal preload force, $F_{z0}$, is exerted by providing normal deflection offset, $Z_{P0}$, on the AFM probe. Then, the substrate moves with constant velocity and the cluster sticks to it and moves with the substrate (Figure 1(g)). The lateral motion of the cluster helps to increase the pushing force, $FT$. Finally, the pushing force reaches the magnitude of the critical force required to overcome the adhesion forces between the cluster and substrate. The cluster's movement with the substrate stops when the cluster has reached the desired position (End of part (G) and start of part (H) of Figure 1). At this time, depending on the dynamic mode diagram of the cluster, the suggested behavior will be expected from the cluster. The probe moves upward (Figure 1(h)) and goes to the initial reference position when the process is completed (Figure 1(i)).

The pushing force imposes a deflection along the path of movement during the manipulation. Based on the cluster substrate properties and the pushing force, three different deflection results can be expected (Figure 2). Although rigid clusters can be moved without deformation (Figure 2(a)),

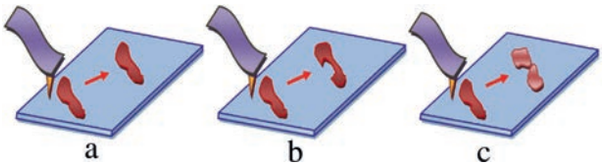


Figure 2: Three expected results: (a) rigid nano cluster, (b) flexible nano cluster, (c) soft nano cluster.

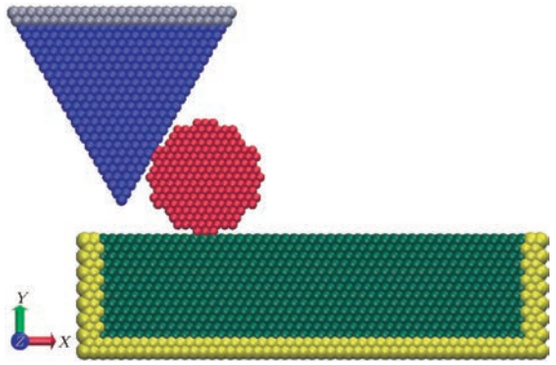


Figure 3: Nano manipulation system configuration.

flexible clusters may undergo considerable deformation during the moving process (Figure 2(b)), and the soft clusters may be damaged when the pushing force exceeds the yield strength of the cluster (Figure 2(c)).

Based on the proposed manipulation strategy, a macro and molecular model are simulated and compared. Using the appropriate atomic potential, in the molecular model, the foregoing forces are modeled implicitly, whereas in the macro model, they are exerted explicitly.

### 3.1. Simulation procedure

Figure 3 shows the initial system configuration for the nano manipulation procedure. The problem is considered as a 2D manipulation of the nano cluster in the *xy* plane. Therefore, the atom's movement is limited to the *xy* plane. For reducing the relaxation phase time, in which atoms take their minimum potential energy positions, the initial positions of atoms are arranged in a hexagonal network. After the relaxation phase, the nano cluster is subjected to the proposed nano manipulation strategy. The manipulator, which is part of an AFM tip, starts moving with constant velocity, dictated by the constant velocity of the uppermost atoms. The manipulator is flexible, so, the blue atoms can move in both the *x* and *y* directions, and make different vibration modes along the tip length. The substrate is flexible as well; however, the yellow atoms (as depicted in Figure 3) are fixed to avoid movement during manipulation. The manipulator, nano cluster, and substrate can be made of a variety of materials (Table 1). The aim of the performed simulation is to study the effect of tip flexibility on the success of the proposed manipulation strategy.

As mentioned before, simulation of considerable size and time cannot be achieved using the molecular dynamics method. However, some techniques are available for modeling sizes and times greater than in the molecular dynamic case. Coarse Grained Molecular Dynamics (CGMD) is a good procedure for this purpose. The time step for the simulations is 80 fs.

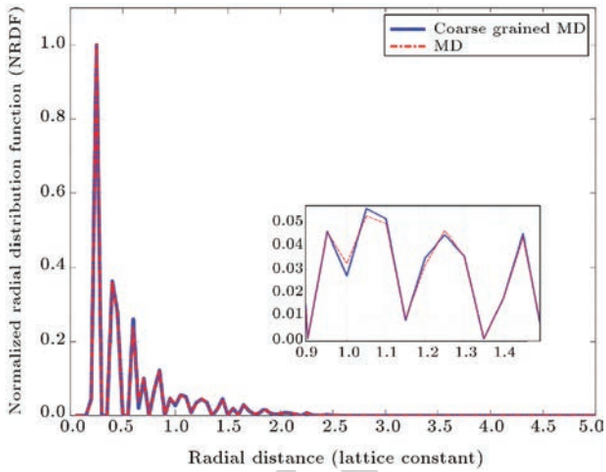


Figure 4: Comparison between RDFs of the MD and CGMD models.

## 4. Coarse Grained Molecular Dynamics (CGMD)

Electromechanical processes normally occur in the order of nano, micro, milli, and, even, a few seconds. In addition, they have higher-than-nano dimensions, and, therefore, their real dimensions and time ranges cannot be determined through the use of the molecular dynamics method. However, by the use of "coarse graining", larger dimensions, in longer time ranges, could be modeled. Now, since a remarkable method, known as Coarse Grained Molecular Dynamics (CGMD), has been presented for this purpose, during its application, a general description of this approach is also provided. The CGMD method is based on the notion that, if, instead of one atom, a larger number of atoms can be taken as a unit, then, a larger volume of material, as well as longer simulation time, can be considered. Even by utilizing the world's largest and most advanced supercomputers, the molecular dynamics simulations cannot be performed for more than several microseconds. Various procedures have been proposed for the CGMD methods [27–29]. The only crucial issue in these models is the manner of predicting and estimating the system's potential. Achieving a good potential for the system can be guaranteed through a process of trial and error, and by comparing the Radial Distribution Function (RDF) of the system with that observed in the MD process; however, other ways also exist for this achievement. If, on average, the nominal mass and distance of atoms are in the order of $m_c$ and $L_c$, and the nominal mass and distance of the CGMD samples are in the order of $m$ and $L$, respectively, the following relations could be considered for the time steps that are used:

$$\Delta t_{\max}|_{MD} \sim l\sqrt{\frac{m}{kT}}, \qquad \Delta t_{\max}|_{CGMD} \sim l_c\sqrt{\frac{m_c}{kT}}. \tag{19}$$

In this paper, for using the CGMD approach, the Sutton–Chen potential has been rewritten, the RDF diagrams of two cases of MD and CGMD have been compared with each other, and the obtained CGMD model has been validated. Figure 4 shows the comparison between the RDFs of the two noted cases. Each interacting site consists of 10 atoms in the CGMD model.

### 4.1. Results and discussions

Using the proposed model, significant results have been achieved. Although all the obtained results cannot be presented,

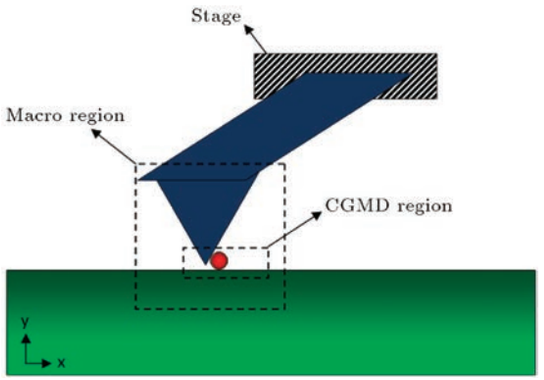


Figure 5: Macro and CGMD regions.

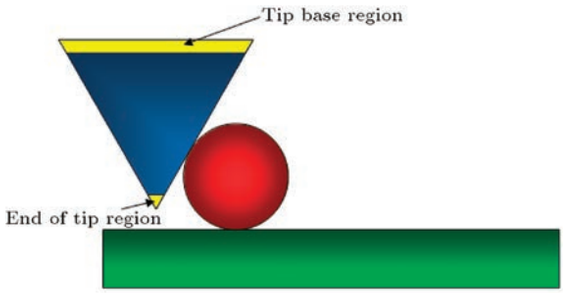


Figure 6: Geometry of tip and nano cluster in CGMD model.

it is attempted to include the most important and applicable results in this article. To validate the obtained results, it is necessary to compare them with already verified results. For this purpose, the results of the present work are compared with those obtained from the model presented in [20,21].

*4.1.1. A comparison of CGMD and macro models*

For the sake of comparison and validation, the macro model in [20,21], which was verified by the available (theoretical and experimental) results, is modified and used for the case of nano cluster manipulation. By implementing some changes to the macro model, it can be reliably generalized to nano cluster manipulation processes.

Using coarse grained molecular dynamics, a comparison has been made between the results of the proposed model and those of the modified macro model. The system geometry has been depicted in Figures 5 and 6. The tip, nano cluster and substrate are made of Ag, Ni and Au, respectively. The nano cluster has the same size in both models, but the substrate and the tip are considered as depicted in Figure 5.

*In the CGMD model*, the substrate, nano cluster and, more importantly, the manipulator tip, are considered to be flexible to ensure real conditions. The initial and final states of the proposed CGMD model are depicted in Figure 7.

*In the macro model*, the manipulation procedure has been simulated by giving the base of the AFM tip (i.e. the stage in Figure 5) a constant speed along the '*x*' direction. The manipulator is the triangular tip of the AFM, which is considered to be rigid. The deflections of the AFM tip, when manipulating the nano cluster, is due to the flexibility of the AFM cantilever. The nano cluster is considered to have a spherical shape, and no flexibility (it is rigid). The nano scale interactions between the substrate and nano cluster are modeled with the JKR contact model. At the start of the

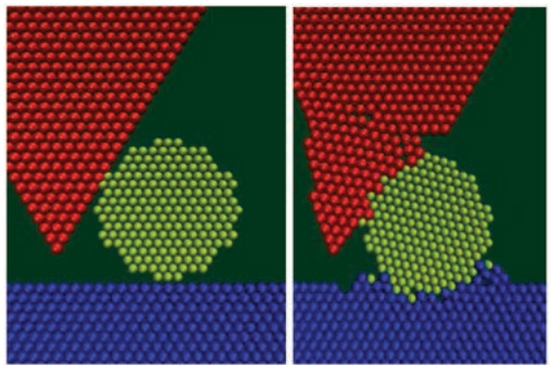

Figure 7: Initial and final states of nano manipulation process for CGMD Macro comparison.

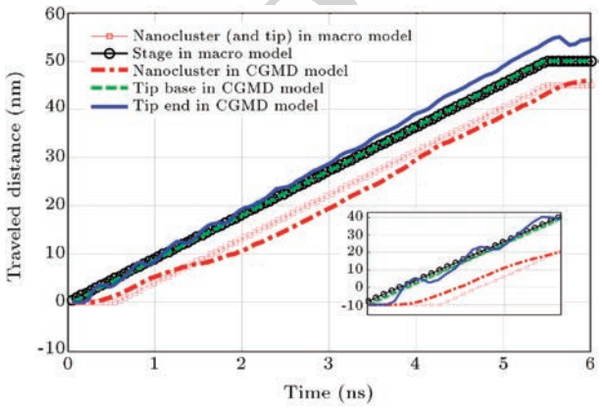


Figure 8: Comparison between the results of macro model and coarse grained molecular dynamics (CGMD) model for the manipulation of nano clusters. (For interpretation of the references to colour in this figure legend, the reader is referred to the web version of this article.)

manipulation procedure, it takes a few seconds for the nano cluster (and AFM tip) to start moving, because the pushing force is not large enough to overcome the resistant frictional force. Once the movement starts, the AFM tip and nano cluster are assumed to move together and, therefore, trace the same line in the traveled distance-time diagram.

Considering the fact that in the macro model, the tip and cluster are assumed to be rigid and the force is supposed to be applied from the moment the probe contacts the cluster, in Figure 8, the diagram indicated by the red square shows the displacement of the cluster and probe tip, and the diagram indicated by the black circle, shows the displacement of the moving substrate. The comparison of these diagrams with the results obtained from the CGMD model has yielded very interesting results. As observed in Figure 8, there is relatively good agreement between the diagrams of the model proposed in this article and the results of the macro model. There are also some differences, which have arisen from the higher accuracy of the CGMD model, as well as the imprecise assumptions of the macro model.

There are several important points regarding the above diagrams. The macro model has focused on estimation of the time of nano cluster movement subsequent to the application of force. In the macro model, after the application of force, the friction forces resist against the exerted force until they get to be equal to the applied force. From this moment on, the cluster starts moving. Therefore, the frictional characteristics

that are considered between the cluster and substrate could be very important in determining this manipulation time. In the CGMD model, we do not necessarily impose any specific frictional characteristics on the model. It is the forces arising from the potentials between dissimilar atoms, and the effects of damping considered in the CGMD model that play the most significant roles in determining the time of movement of the nano cluster. In view of the presented diagrams, the CGMD model has underestimated, a little, the time of movement of the nano cluster compared to the macro model. The other noteworthy point is that the amount of traveled distance of the nano cluster is less than that of the tip. This has two major causes: first, the existing delay in the start of nano cluster movement, and second, the initial distance between the probe tip and nano cluster. This short distance is not necessarily due to the initial position of the tip, but may be the result of initial deformations of the tip end.

In the enlarged portion of the diagram in Figure 8, it is clear that, at the onset of cluster movement, the tip end vibrates in the CGMD, which is due to local attraction and repulsion between the tip end and cluster, and also due to the immediate application of velocity at the tip base. Of course, as a result of the damping effect and also the local equilibrium of potentials, these vibrations are gradually eliminated. With regards to the comparisons and offered explanations, the correctness of the results of the proposed model is verified, and it can be used for other studies including the study of the effects of different parameters.

## 5. Some challenges

### 5.1. Tip deformations

Although, for the conditions presented in the previous section, a successful manipulation has been performed, as occurs in real operations, the adjustment of a successful nano manipulation process is very difficult. In some cases, the process fails because of the damage of the tip. In some other cases, the nano cluster deeply penetrates the substrate surface, or is crushed. At any rate, to tune the parameters for a successful manipulation operation, we need to have enough experience and spend a relatively long time on the problem. Several examples of these failures are presented in the following sections. In each section, only the final moment of the nano manipulation process has been illustrated. Tip damage is one of the causes of unsuccessful nano manipulation process. This phenomenon leads to the formation of crack in the tip, permanent deformation of the tip end, or even in some cases, the fracture of the tip. Some examples of this phenomenon have been portrayed in Figure 9. In Figure 10, the desired displacement and also the displacements of the nano cluster and tip end, as a result of tip deformation, have been plotted. The deviation of the nano cluster manipulation curve from the desired curve can be clearly seen.

### 5.2. Cluster deformations

Although, in most cases, tip deformation is highly important and crucial, in certain cases, such as the manipulation of biological nanoobjects, the deformation (crushing) of the cluster could also be significant (see Figures 11 and 12). Some examples of nano cluster deformation during the process of nano manipulation can be seen in Figure 11. The desired displacement and also the displacements of the nano cluster

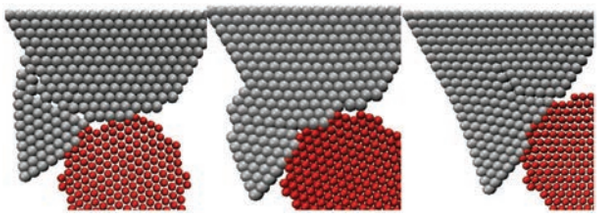

Figure 9: Some examples of tip damage.

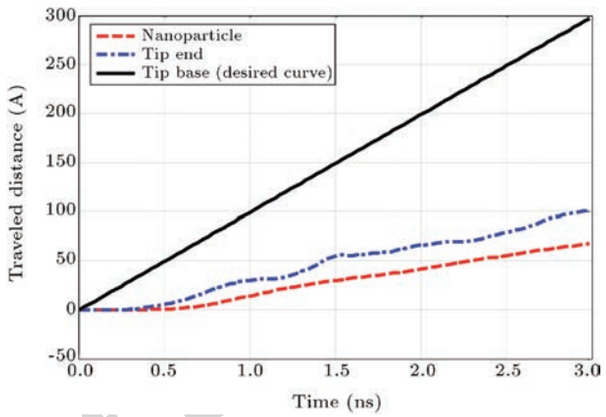


Figure 10: Traveled distances of the tip end, nano cluster, and tip base in the case of tip damage.

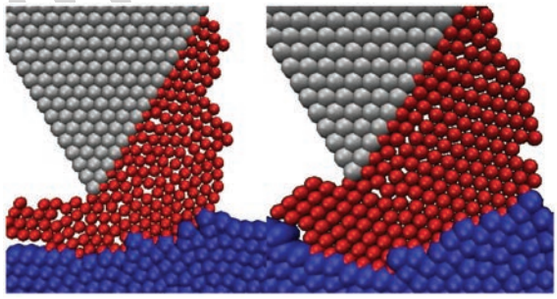

Figure 11: Examples of the crushing of nano cluster.

and tip end, as a result of cluster deformation, have been plotted (Figure 12). Although the tip end roughly follows the movement of the tip base, the deviation of the nano cluster manipulation curve from the desired curve can be clearly seen.

### 5.3. Surface related challenges

Elastic and viscoelastic substrates are other factors that may lead to flawed and incorrect manipulation results. Figures 13 and 14 show the effects of a highly compliant substrate surface (with large deformation) on the manipulation of nano clusters. An example of nano cluster deformation in the process of nano manipulation can be observed in Figure 13. In Figure 14, the desired displacement and also the displacements of the nano cluster and tip end as a result of cluster deformation, have been plotted. Although the tip end roughly follows the movement of the tip base, after the tip base is displaced, the substrate is indented by the cluster, and the kinetic energy of the cluster is spent on the internal deformation of the substrate. Thus, the cluster's speed and displacement are reduced.

Normally, substrate surfaces on which the manipulation process takes place are hard metal surfaces, and the intention

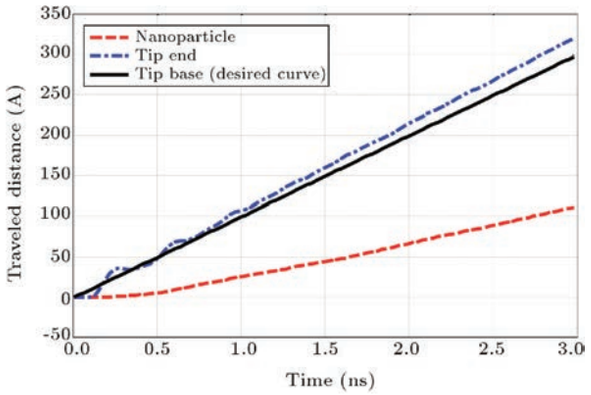


Figure 12: Traveled distances of the tip end, nano cluster, and tip base for the case of crushed nano cluster.

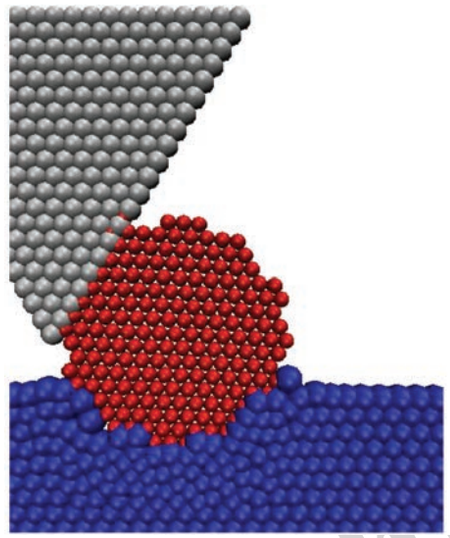

Figure 13: An example of nano cluster indentation into the substrate.

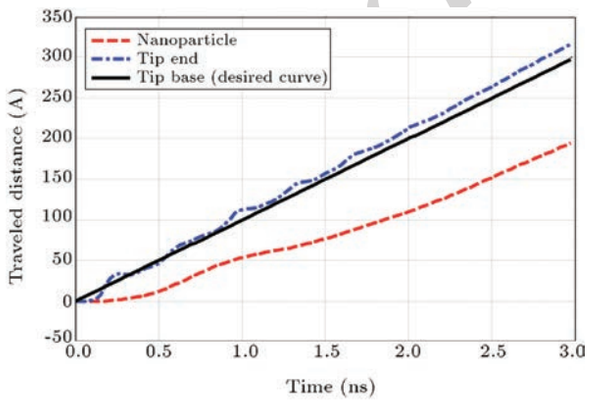


Figure 14: Traveled distances of the tip end, nano cluster, and tip base for the case of substrate indentation.

has been the manipulation of metal nano clusters. In view of the diagrams of this section, it seems that from among the aforementioned damage, after tip damage, the crushing of the cluster has the most negative impact on the successful accomplishment of the nano manipulation process, because the deviation of the nano cluster's position from the desired

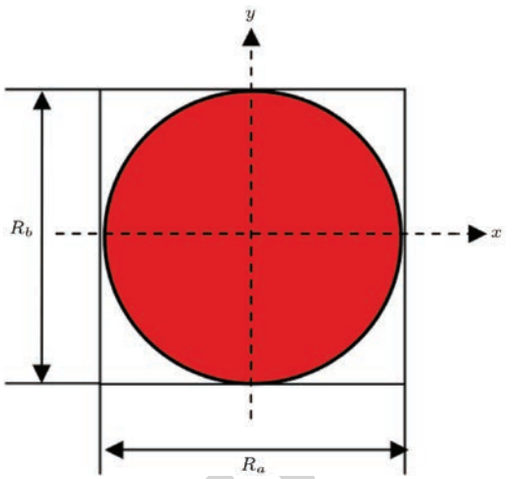


Figure 15: Initial form of the nano cluster with equal diameters of $R_a$ and $R_b$.

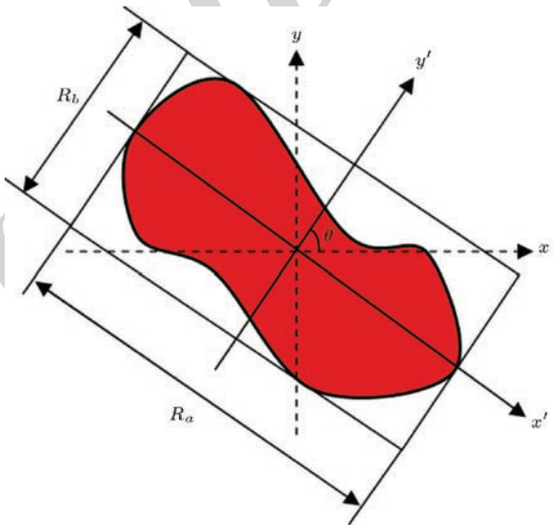


Figure 16: General case of the nano cluster box with unequal diameters of $R_a$ and $R_b$.

position is relatively large. Therefore, in the following sections, the effects of several factors responsible for cluster crushing will be thoroughly discussed.

### 5.4. Effects of parameters on nano cluster deformation

In this part, the effects of two parameters on the success of the manipulation procedure have been studied. These parameters are: $\varepsilon_p$ (Sutton–Chen coefficient for the cluster) and $\varepsilon_t$ (Sutton–Chen coefficient for the tip). The criterion considered for the success of the manipulation process, called the Success Parameter (SP), is defined as the change in the ratio of two equal orthogonal radii of the nano cluster.

$$SP = \frac{R_a}{R_b}. \tag{20}$$

$R_a$ and $R_b$ have been depicted in Figures 15 and 16, respectively.

When the nano cluster is spherical, the SP ratio will be equal to 1.0, and, as the nano cluster deforms, the value of SP will deviate from 1.0. Although this parameter indicates cluster deformation, in some rare cases also (while the nano cluster has

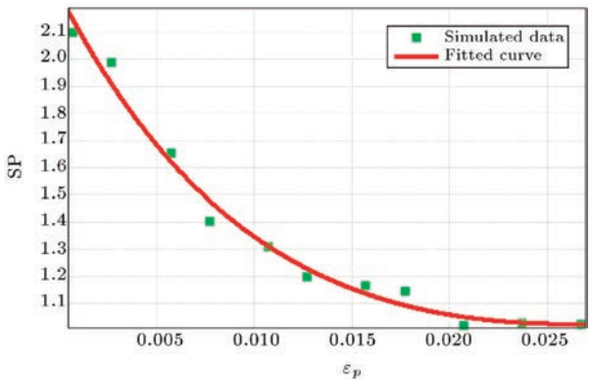


Figure 17: Data and the fitted SP curve with the change of $\varepsilon_p$.

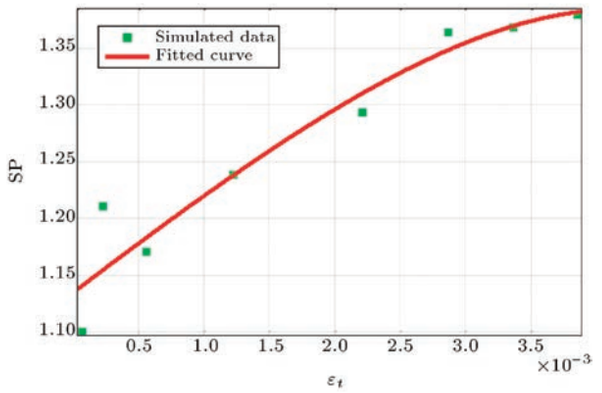


Figure 18: Data and the fitted SP curve with the change of $\varepsilon_t$.

Table 2: Results of various simulations with the change of $\varepsilon_p$ and $\varepsilon_t$.

| (A) Values of SP with the change of $\varepsilon_p$ (Ag tip: $\varepsilon_t = 2.5415E-03$) | | (B) Values of SP with the change of $\varepsilon_t$ (Cu nano cluster: $\varepsilon_p = 1.2382E-02$) | |
|---|---|---|---|
| $\varepsilon_p$ | SP | $\varepsilon_t$ | SP |
| 0.000707 | 2.0981 | 0.0000684 | 1.1000 |
| 0.002707 | 1.9872 | 0.0002333 | 1.2104 |
| 0.005707 | 1.6512 | 0.000563 | 1.1710 |
| 0.007707 | 1.4046 | 0.0012225 | 1.2389 |
| 0.010707 | 1.3083 | 0.0022118 | 1.2937 |
| 0.012707 | 1.1969 | 0.0028712 | 1.3640 |
| 0.015707 | 1.1670 | 0.0033659 | 1.3681 |
| 0.017707 | 1.1448 | 0.0038605 | 1.3790 |
| 0.020707 | 1.0195 | | |
| 0.023707 | 1.0245 | | |
| 0.026707 | 1.0232 | | |

deformed and its shape is no longer spherical), this parameter might be equal to 1.0. In any case, as far as the change of the nano cluster box is concerned, with regards to Figure 16, the change of nano cluster shape can be generally defined as Relation (20).

For a general case, $R_a$ is the distance between the farthest atoms. The $x'$ axis is defined along these atoms. With a coordinate transformation from the $xy$ axes to $x'y'$, $R_b$ is defined as the distance between the highest and lowest points in the $y'$ direction. Using these definitions, all atoms are swept with a rectangle of area $R_aR_b$.

Since cluster deformation is one of the crucial parameters in the success of a nano manipulation process, to analyze and evaluate this phenomenon, a new parameter called SP has been introduced. This parameter can be very useful in the displacement of biological clusters, particularly in the manipulation and making of special biological objects.

Table 2 summarizes the results of different simulations with various amounts of $\varepsilon_p$ and $\varepsilon_t$. The base materials of the tip and nano cluster are copper (Cu) and silver (Ag), respectively. The substrate is made of Au. By fitting an exponential curve in the form of $y = ae^{bx} + ce^{dx}$ to the case A data of Table 2, the values of 1.697, 88.73, 0.545, and 17.29 are obtained for the coefficients, $a$, $b$, $c$, and $d$, respectively. The $R$ square value of this curve is equal to 0.986. The data and the fitted curve have been shown in Figure 17.

As in the previous case, by fitting an exponential curve in the form of $y = ax^b + c$ to the case B data of Table 2, the values of 6.41, 0.5563, and 1.095 are obtained for the coefficients, $a$, $b$, and $c$, respectively. The $R$ square value of this curve is equal to 0.9318. The data and the fitted curve have been shown in Figure 18.

Figure 17 shows that, with an increase in the $\varepsilon_p$ coefficient, the value of the SP parameter, and consequently, the deformation of the cluster, decreases. The increase of the SP increases the cohesion of the nano cluster's atoms and, therefore, $\varepsilon_p$ is proportionate to the hardness of the cluster, and the obtained result is very reasonable. Also, it can be observed in Figure 18 that in general, with an increase in $\varepsilon_t$, the SP parameter and, consequently, the cluster deformation, increases, although the local data changes do n,ot necessarily have an ascending trend. At any rate, the increase of the SP is not favorable to the nano manipulation process. It seems that tip flexibility (softness of the tip) can be beneficial for not deforming the nano cluster, as long as it does not hinder the other objectives of the manipulation. This conclusion also seems reasonable, because part of the energy which is supposed to deform the nano cluster will be absorbed through the deformation of the tip, and the nano cluster will remain more rigid.

### 5.5. The tip cluster $\varepsilon$ — SP diagram

Some simulations for the manipulation of several different clusters have been performed by using various manipulator tips. The following diagram (Figure 19) covers all the metals of the Sutton–Chen table. By using this diagram, one can easily select the appropriate manipulator tip for the considered nano cluster, so that the smallest SP number, and thus, the least amount of physical change could be resulted. As an example, if the considered nano cluster is made of gold, it is suggested that a platinum tip be selected. The use of a silver tip is the worst choice, and will result in relatively large deformations of the nano cluster. These facts can be also concluded from the data of Table 3, which lists the value of SP number versus the change of $\varepsilon_p$ and $\varepsilon_t$ (i.e. the change of cluster and tip materials). In the foregoing example for the gold nano cluster, use of the platinum tip would lead to the least SP number (i.e. 1.111) and use of the silver tip would lead to the highest SP number (i.e. 1.225).

## 6. Conclusion

In the present paper, the manipulation of nano clusters with a flexible AFM tip was modeled using the CGMD model, and the effects of different parameters on the success of the nano manipulation procedure were studied. To validate the

Table 3: The values of SP number with the changes of $\varepsilon_p$ and $\varepsilon_t$.

| Cluster material ($\varepsilon_p$) | Tip material ($\varepsilon_t$) | | | | |
|---|---|---|---|---|---|
| | Ag (2.5415E−3) | Rh (4.9371E−3) | Au (1.2793E−2) | Pt (1.9833E−2) | Al (3.3147E−2) |
| Ir (2.4489E−3) | 1.934 | 1.861 | 2.035 | 1.903 | 1.869 |
| Ag (2.5415E−3) | 1.925 | 1.846 | 2.006 | 1.86 | 1.842 |
| Pd (4.1790E−3) | 1.758 | 1.647 | 1.655 | 1.446 | 1.54 |
| Rh (4.9371E−3) | 1.689 | 1.574 | 1.548 | 1.361 | 1.464 |
| Pb (5.5765E−3) | 1.634 | 1.519 | 1.471 | 1.309 | 1.414 |
| Cu (1.2382E−2) | 1.241 | 1.194 | 1.148 | 1.116 | 1.18 |
| Au (1.2793E−2) | 1.225 | 1.184 | 1.141 | 1.111 | 1.173 |
| Ni (1.5707E−2) | 1.137 | 1.129 | 1.106 | 1.088 | 1.135 |
| Pt (1.9833E−2) | 1.06 | 1.083 | 1.076 | 1.069 | 1.098 |
| Al (3.3147E−2) | 1.024 | 1.018 | 1.009 | 1.042 | 1.037 |

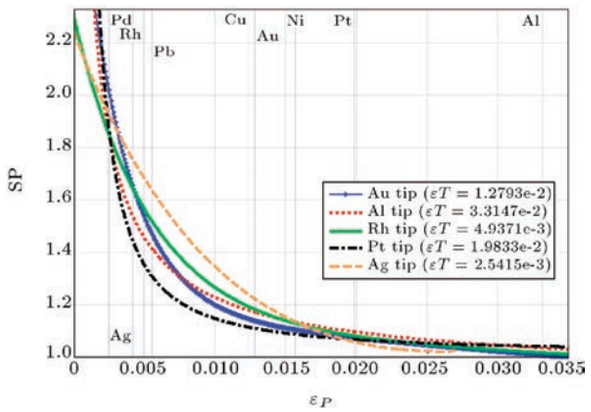


Figure 19: Change of SP parameter versus the changes of $\varepsilon_t$ and $\varepsilon_p$.

proposed model, it has been compared with the results of previous work. Although for all the conditions presented in this paper, a successful manipulation has been performed, as occurs in real cases, the adjustment of a successful nano manipulation process is very difficult. To show the failures of the manipulation process, some examples of these failures were presented, and it was shown that nano cluster crushing was one of the most crucial failures, which must be taken deeply into consideration in real manipulation systems. Investigations were, therefore, conducted on the effect of different parameters on the deformation of the nano cluster to study the success of the manipulation procedure. It was observed from the obtained results that by increasing $\varepsilon_p$ and $\varepsilon_t$ (the parameters of Sutton–Chen potential for nano cluster and tip) coefficients, the cluster deformation decreases and increases, respectively. The obtained result is reasonable, since the increase of $\varepsilon_p$ increases the cohesion of the nano cluster's atoms and, thus, $\varepsilon_p$ is proportional to the hardness of the cluster. It seems that tip flexibility (softness of tip) can be beneficial, in order to avoid deformation of the nano cluster, as long as it does not hurt the other objectives of the manipulation. This conclusion also seems reasonable, because part of the deformation energy of the nano cluster will be absorbed through tip deformation, and the nano cluster will remain more rigid. Moreover, for the benefit of designers and manufacturers of nanomanipulator systems, a diagram was developed, in which, the simultaneous effects of $\varepsilon_p$ and $\varepsilon_t$ parameters on the success of manipulation of nano cluster have been shown. If the nano cluster material is known, by using the diagrams of Figure 19, the optimal selection of the tip, which causes the least deformation in the nano cluster and leads to the best positioning result, can be obtained.

## Acknowledgment

The authors sincerely thank Mr. Mahdi Moradi for his cooperation in the validation part of this work.

## References

[1] Griebel, M., Knapek, S. and Zumbusch, G., *Numerical Simulation in Molecular Dynamics, Numerics, Algorithms, Parallelization, Applications*, Springer (2007).
[2] Rapaport, D.C., *The Art of Molecular Dynamics Simulation*, Cambridge University Press (2004).
[3] Liu, W.K., Karpov, E.G. and Park, H.S., *Nano Mechanics and Materials Theory, Multiscale Methods and Applications*, John Wiely & Sons (2006).
[4] Korayem, M.H., Sadeghzadeh, S. and Homayooni, A. "Semi analytical motion analysis of nano steering devices, segmented piezotube scanners", *Int. J. Mech. Sci.*, 53(7), pp. 536–548 (2011).
[5] Peng, J.S., Yuan, Y.Q., Yang, J. and Kitipornchai, S. "A semi analytic approach for the nonlinear dynamic response of circular plates", *Appl. Math. Model.*, 33, pp. 4303–4313 (2009).
[6] Hsu, H. "Electromechanical analysis of electrostatic nano actuators using the differential quadrature method", *Commun. Numer. Methods Eng.*, 24(11), pp. 1445–1457 (2008).
[7] Sitti, M. "Survey of nano manipulation systems", *IEEE Nanotechnology Conference*, Maui, USA, pp. 75–80 (2001).
[8] Tafazzoli, A. and Sitti, M. "Dynamic modes of nano particle motion during nanoprobe based manipulation", *Proc. of 4th IEEE Conf. on Nanotechnology*, Munich, Germany, pp. 35–37 (2004).
[9] Sitti, M. "Controlled pushing of nanoparticles: Modeling and experiments", *IEEE/ASME Trans. on Mechat.*, 5(2), pp. 199–211 (2000).
[10] Zhang, J., Li, G. and Xi, Ning "Modeling and control of active end effector for the AFM based nano robotic manipulators", *11th Int. Conf. on Rob. and Aut., Barcelona*, Spain, pp. 163–168 (2005).
[11] Derjaguin, B.V., Muller, V.M. and Toporov, Yu.P. "Effect of contact deformations on the adhesion of particles", *J. Colloid Interface Sci.*, 53(2), pp. 314–326 (1975).
[12] Quesnel, D.J., Rimai, D.S. and Demejo, L.P. "Molecular dynamic simulation of adhesional release of particles from surfaces", *J. of Adh.*, 67, pp. 235–257 (1998).
[13] Jay Chey, S., Huang, L. and Weaver, J.H. "Interface bonding and manipulation of Ag and Cu nanocrystals on Si (111) (7∗7) based surfaces", *Phys. Rev. B*, 59(24), pp. 16033–16041 (1999).
[14] Lagoute, J., Kanisawa, K. and Fölsch1, S. "Manipulation and adsorption site mapping of single pentacene molecules on Cu(111)", *Phys. Rev. B*, 70(245415), pp. 1–6 (2004).
[15] Hertel, T., Walkup, R.E. and Avouris, Ph "Deformation of carbon nanotubes by surface van der Waals forces", *Phys. Rev. B*, 58(20), pp. 13870–13873 (1998).
[16] Rollot, Y., Regnier, S. and Guinot, J.C. "Simulation of micro manipulations: adhesion forces and specific dynamic models", *Int. J. of Adhesion & Adhesives*, 19, pp. 35–48 (1999).
[17] Luedtke, W.D. and Landman, U. "Stability and collapse of metallic structures on surfaces", *Phys. Rev. Lett.*, 73(4), pp. 569–572 (1994).
[18] Mahboobi, S.H., Meghdari, A., Jalili, N. and Amiri, F. "Qualitative study of nano cluster positioning process: Planar molecular dynamics simulations", *Curr. Appl. Phy.*, 9, pp. 997–1004 (2009).
[19] Mahboobi, S.H., Meghdari, A., Jalili, N. and Amiri, F. "Qualitative study of nanoassembly process: 2 D molecular dynamics simulations", *Sci. Ira. J., Trans. on Nano. F*, 17(1), pp. 1–11 (2010).

[20] Moradi, M., Freidon, A.H. and Sadeghzadeh, S. "Aspect ratio and dimension effects on nanorod manipulation by Atomic Force Microscope (AFM)", *Micro and Nano Lett.*, 5(5), pp. 324–327 (2010).
[21] Moradi, M., Freidon, A.H. and Sadeghzadeh, S. "Dynamic modeling for nano manipulation by AFM: polystyrene nanorod case study", *Sci. Ira. J., Trans. on Nano. F*, 18(3), pp. 808–815 (2011).
[22] Rahneshin, V. "Dynamic modeling of nanostructures manipulation based on multiscale methods", M.Sc. Thesis, Iran University of Science and Technology (IUST), Iran (2011).
[23] Allen, M.P. and Tildesley, D.J., *Computer Simulation of Liquids*, Clarendon Press (1987).
[24] Rafii Tabar, H. "Modeling the nano scale phenomena in condensed matter physics via computer based numerical simulation", *Phys. Rep.*, 325, pp. 239–310 (2000).
[25] Sutton, A.P. and Chen, J. "Long range Finnis Sinclair potentials", *Phil. Mag.*, 61, pp. 139–146 (1990).
[26] Requicha, A.G., *Nanorobotics: Handbook of Industrial Robotics*, 2nd Edn., John Wiley and Sons pp. 199–210 (1999).
[27] Marrink, S.J., de Vries, A.H. and Mark, A.E. "Coarse grained model for semiquantitative lipid simulations", *J. Phy. Chem. B*, 108, pp. 750–760 (2004).
[28] Rudd, R.E. and Broughton, J.Q. "Coarse grained molecular dynamics: nonlinear finite elements and finite temperature", *Phys. Rev. B*, 72, pp. 104–144 (2005).
[29] Li, Xiantao "A coarse grained molecular dynamics model for crystalline solids", *Int. J. Numer. Methods Eng.*, 83, pp. 986–997 (2010).

**Moharam Habibnejad Korayem** was born in Tehran, Iran, in 1961. He received his B.S. (Hon) degree and his M.S. degree in Mechanical Engineering from Amirkabir University of Technology in 1985 and 1987, respectively, and his Ph.D. degree in Mechanical Engineering from the University of Wollongong, Australia, in 1994. He is a Professor of Mechanical Engineering at Iran University of Science and Technology, Iran, where, for the last 17 years, he has been involved with teaching and research activities in the area of robotics. His research interests include: dynamics of elastic mechanical manipulators, trajectory optimization, symbolic modeling, robotic multimedia software, mobile robots, industrial robotics standards, robot vision, soccer robot, and the analysis of mechanical manipulator with maximum load carrying capacity.

He has published and presented more than 370 papers in international journals and at conferences in his area of expertise.

**Vahid Rahneshin** received his B.S. degree from Ferdowsi University of Mashhad, in 2009, and is now an M.S. degree student at Iran University of Science and Technology, where he is also a member of the Robotics Research Laboratory. His research interests include: nano/micro mechanics and computational methods in solid mechanics.

**Sadegh Sadeghzadeh** received his B.S. and M.S. degrees in Mechanical Engineering from Semnan University and Iran University of Science and Technology (IUST) in 2006 and 2008, respectively. He is presently a Ph.D. degree candidate of Mechanical Engineering at IUST. His research interests include: vibration control, robotics and micro and nano manipulation.